SCIENTIFIC REPORTS

OPEN

Involvement of TRPM2 and TRPM8 in temperature-dependent masking behavior

Wataru Ota [1,2], Yusuke Nakane[1,2], Makiko Kashio[4], Yoshiro Suzuki [5,6], Kazuhiro Nakamura [7], Yasuo Mori[8], Makoto Tominaga[5,6] & Takashi Yoshimura [1,2,3,9]

Masking is a direct behavioral response to environmental changes and plays an important role in the temporal distribution of activity. However, the mechanisms responsible for masking remain unclear. Here we identify thermosensors and a possible neural circuit regulating temperature-dependent masking behavior in mice. Analysis of mice lacking thermosensitive transient receptor potential (TRP) channels (*Trpv1/3/4* and *Trpm2/8*) reveals that temperature-dependent masking is impaired in *Trpm2*- and *Trpm8*-null mice. Several brain regions are activated during temperature-dependent masking, including the preoptic area (POA), known as the thermoregulatory center, the suprachiasmatic nucleus (SCN), which is the primary circadian pacemaker, the paraventricular nucleus of the thalamus (PVT), and the nucleus accumbens (NAc). The POA, SCN, PVT are interconnected, and the PVT sends dense projections to the NAc, a key brain region involved in wheel-running activity. Partial chemical lesion of the PVT attenuates masking, suggesting the involvement of the PVT in temperature-dependent masking behavior.

The circadian clock, a 24-hour endogenous biological timer, is highly conserved in virtually all living organisms. This clock regulates various physiological and behavioral processes, such as sleep–wake cycles and metabolism. Entrainment and masking are two independent processes that determine whether animals exhibit diurnal or nocturnal behavior[1,2]. Entrainment refers to synchronization of the circadian clock to environmental cycles, whereas masking is a direct response to environmental signals with a change in activity. Interplay between entrainment and masking results in the distribution of locomotor activity to a specific time of day, known as the temporal niche. Entrainment of circadian rhythms is mediated by light information received by rods, cones, and melanopsin (OPN4)-expressing retinal ganglion cells. This information is then conveyed to the suprachiasmatic nucleus (SCN), the central circadian pacemaker located in the hypothalamus, directly via the retinohypothalamic tract (RHT) and indirectly from the intergeniculate leaflet (IGL) via the geniculo-hypothalamic tract (GHT)[3–6]. Thus, the photoreceptors and neural circuits involved in photoentrainment are well established. In marked contrast, the mechanism(s) responsible for masking behavior remain unclear.

Non-mammalian vertebrates perceive light information directly within the brain via deep brain photoreceptors[7]. In previous studies, we found that OPN5-positive cerebrospinal fluid (CSF)-contacting neurons within the hypothalamus are among the deep brain photoreceptors that regulate seasonal reproduction in birds[8,9].

[1]Institute of Transformative Bio-Molecules (WPI-ITbM), Nagoya University, Furo-cho, Chikusa-ku, Nagoya, 464-8601, Japan. [2]Laboratory of Animal Integrative Physiology, Graduate School of Bioagricultural Sciences, Nagoya University, Furo-cho, Chikusa-ku, Nagoya, 464-8601, Japan. [3]Avian Bioscience Research Center, Graduate School of Bioagricultural Sciences, Nagoya University, Furo-cho, Chikusa-ku, Nagoya, 464-8601, Japan. [4]Department of Physiology, Aichi Medical University, 1-1 Yazakokarimata, Nagakute, 480-1195, Japan. [5]Division of Cell Signaling, National Institute for Physiological Sciences, National Institutes of Natural Sciences, 5-1 Higashiyama, Myodaiji, Okazaki, 444-8787, Japan. [6]Thermal Biology Group, Exploratory Research Center on Life and Living Systems, National Institutes of Natural Sciences, 5-1 Higashiyama, Myodaiji, Okazaki, 444-8787, Japan. [7]Department of Integrative Physiology, Nagoya University Graduate School of Medicine, 65 Tsurumai-cho, Showa-ku, Nagoya, 466-8550, Japan. [8]Department of Synthetic Chemistry and Biological Chemistry, Graduate School of Engineering, Kyoto University, Nishikyo-ku, Kyoto, 615-8510, Japan. [9]Division of Seasonal Biology, National Institute for Basic Biology, National Institutes of Natural Sciences, 38 Nishigonaka, Myodaiji, Okazaki, 444-8585, Japan. Correspondence and requests for materials should be addressed to T.Y. (email: takashiy@agr.nagoya-u.ac.jp)

Interestingly, light also penetrates the brain of some mammalian species[10], and OPN5 is expressed in the mouse and human brain[11,12]. However, the physiological function of OPN5 within the mammalian brain is unknown.

In an effort to understand the physiological function of OPN5 in the mouse brain and test for the possible existence of extra-ocular photoreception in mice, we serendipitously observed suppression of locomotor activity in blinded mice. Further experiments demonstrated that the phenomenon we observed was, in fact, temperature-dependent masking behavior. We went on to identify two thermosensors (TRPM2 and TRPM8), which regulate this adaptive behavior by analyzing all available transient receptor potential (TRP) channel–null mice (*Trpv1/3/4* and *Trpm2/8*). Moreover, we propose a possible neural circuit that mediates this behavior based on expression analysis of the neuronal activation marker *Fos* and chemical lesions in the brain. In particular, the paraventricular nucleus of the thalamus (PVT) may be an important interface that regulates temperature-dependent masking behavior.

Results

Blinded mice exhibit masking behavior during UVA light exposure.
Since mouse and human OPN5 exhibit absorption maxima in the ultraviolet A (UVA) range (360–380 nm)[12,13], we first examined the effect of UVA light on wheel-running activity of blinded C57BL/6 J mice to investigate whether mice have the capacity for extra-ocular photoreception. As expected, intact mice entrained to LD cycles of both white light and UVA light (Fig. 1a), whereas blinding caused free-running rhythms under both of these lighting conditions (Fig. 1b) (n = 5). These results are consistent with previous reports showing that eyes are the only photoreceptive organ in mammals[14,15]. Surprisingly, however, we observed decreased locomotor activity, an example of negative masking behavior[1,2], in blinded mice during exposure to UVA light (Fig. 1b). Although negative masking was observed in all blinded mice tested, the free-running period and extent of masking varied among individuals. Therefore, to further characterize this variability, we analyzed wheel-running activity in additional blinded mice (n = 23). Although the typical free-running period of C57BL/6 J mice is a bit shorter than 24 hours, blinded mice exhibited a broader range and decreased stability in free-running period (Fig. 1c–e). These variations are likely due to the absence of retinal circadian oscillators, which are normally coupled to and interact continuously with the circadian pacemaker in the SCN[16]. About 70% of blinded mice exhibited masking behaviors immediately after transfer to a UVA-LD cycle (Fig. 1f), whereas the rest of the animals developed masking behaviors gradually. When we examined the onset of masking, we noticed that blinded mice exhibited masking behavior when the onset of UVA light coincided with the middle of the subjective day (i.e., circadian time ~6; circadian time 12 is defined as the time of activity onset in nocturnal animals under constant conditions) (Fig. 1g). Phase-specific negative masking effects in mice have also been reported by Hoffmann[17]. Thus, the variation in the onset of masking behavior appears to depend on the large variation in free-running period caused by blinding. In any event, all animals exhibited masking behavior by 70 days after transfer to a UVA-LD cycle (Fig. 1f).

Temperature stimulus causes negative masking behavior in blinded mice.
Due to the phase-dependency of the onset of masking (Fig. 1g), we next exposed mice to an ultradian 7-hour (3.5/3.5-h) UVA-LD cycle[6,18] (Supplementary Fig. S1a). Because mice cannot entrain their circadian rhythms to this 7-hour periodicity, the light and dark portions of the cycle move across the circadian cycle in this ultradian regime; thus, the pattern of activity under this regime represents masking effects rather than activity controlled by the circadian oscillator. Under this ultradian UVA-LD cycle, blinded mice confined their activity mostly to the dark phase but were active randomly under a white-LD cycle (Fig. 2a–c), consistent with the results shown in Fig. 1. Next, we tested whether this negative masking behavior was light-dependent by injecting India ink under the scalp[19]. This treatment reduced the intensity of light that penetrated the skull to approximately 1/200 of that in intact mice. However, India ink injection did not affect masking behavior (Fig. 2d–f), suggesting that mice were not using information from UVA light. When we examined more carefully the activity rhythms in Fig. 2g, we noticed a time lag between UVA light onset and activity offset. Based on this observation, we speculated that an ambient temperature (T_a) rise induced by UVA light might be causing the masking behavior. Indeed, when we measured temporal changes in T_a inside the light-tight box, we observed a significant increase in T_a following UVA light exposure (Fig. 2g). No such temperature rise was observed under white-LD cycles (Fig. 2h). The concurrence between high T_a (>30 °C) and masking behavior suggested that the T_a change caused by the UVA light apparatus was triggering negative masking.
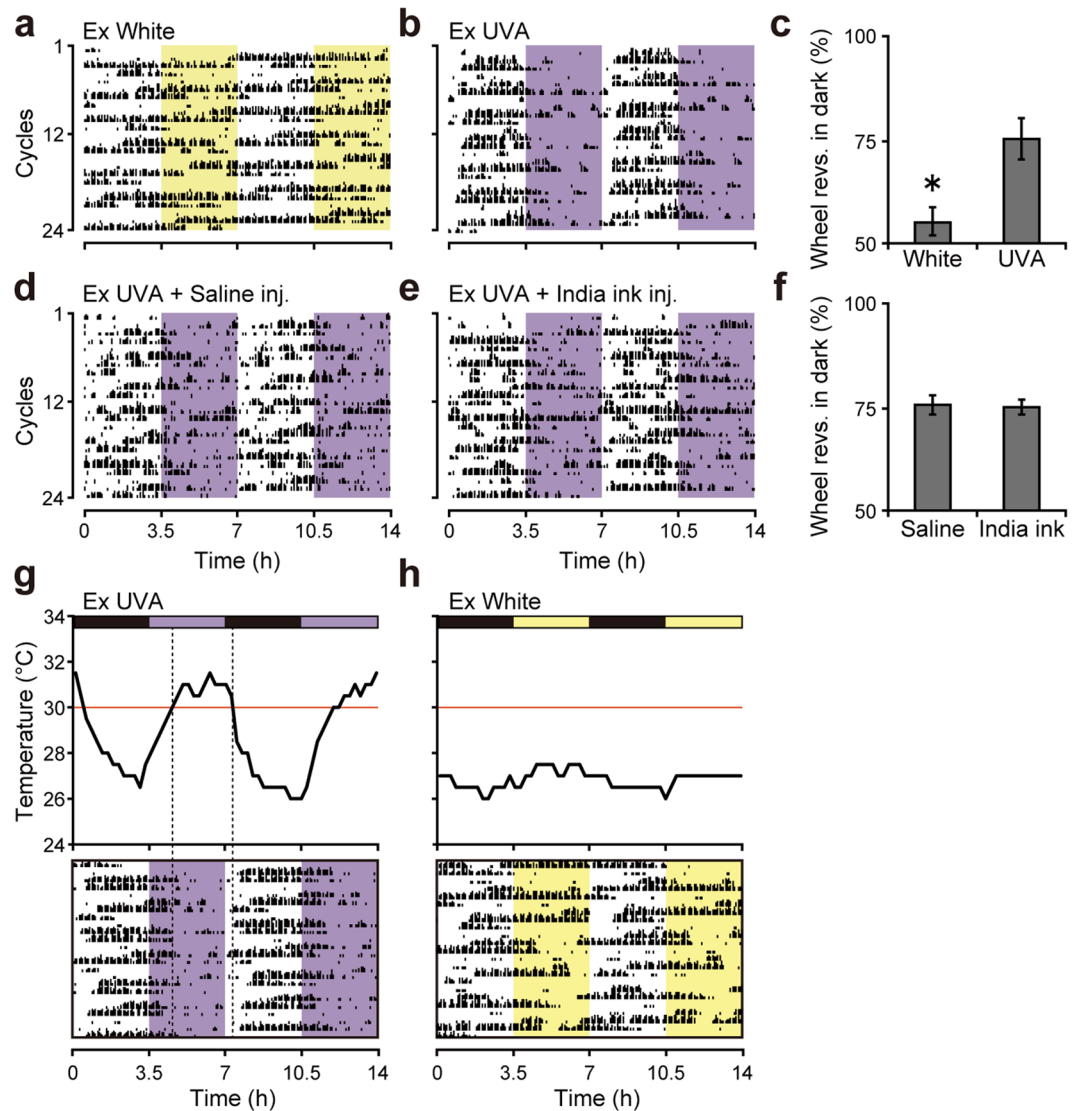
T_a cycles induce negative masking behaviors in mice.
To confirm that T_a cycles were indeed causing the masking behavior, we next examined the effect of various T_a cycles in intact C57BL/6 J mice under constant darkness (DD). In mice, the thermoneutral zone ranges from 26 °C to 34 °C[20,21]. When mice were exposed to 3.5/3.5-hour cycles of various temperature differences (24/24 °C, 24/26 °C, 24/28 °C, 24/30 °C, 24/32 °C, 24/34 °C; Supplementary Fig. S1b), negative masking was observed during exposure to the higher temperature, and the increase in the masking ratio was directly proportional to the increase in the temperature difference (Fig. 3a,b). We also analyzed wheel-running activity rhythms under various T_a cycles in which the difference between maximum and minimum temperature was held constant at 10 °C. Masking behavior was clearer in cycles at higher temperatures (Fig. 3c,d).

Impaired negative masking behavior in *Trpm2* KO and *Trpm8* KO mice.
To date, 10 TRP channels have been identified as thermosensors in mammals[22,23] (Supplementary Fig. S2). TRPA1 and TRPM8 are cold-activated channels, whereas TRPV1, TRPV2, and TRPM3 are heat-activated. On the other hand, TRPV3, TRPV4, TRPM2, TRPM4, and TRPM5 are activated by warm temperatures[22,23]. The thermosensor(s) that mediate temperature-dependent masking behaviors are unknown. To identify these thermosensor(s), we examined masking in all available TRP channel–null mice (*Trpv1/3/4* and *Trpm2/8*) in our laboratory. Because the genetic
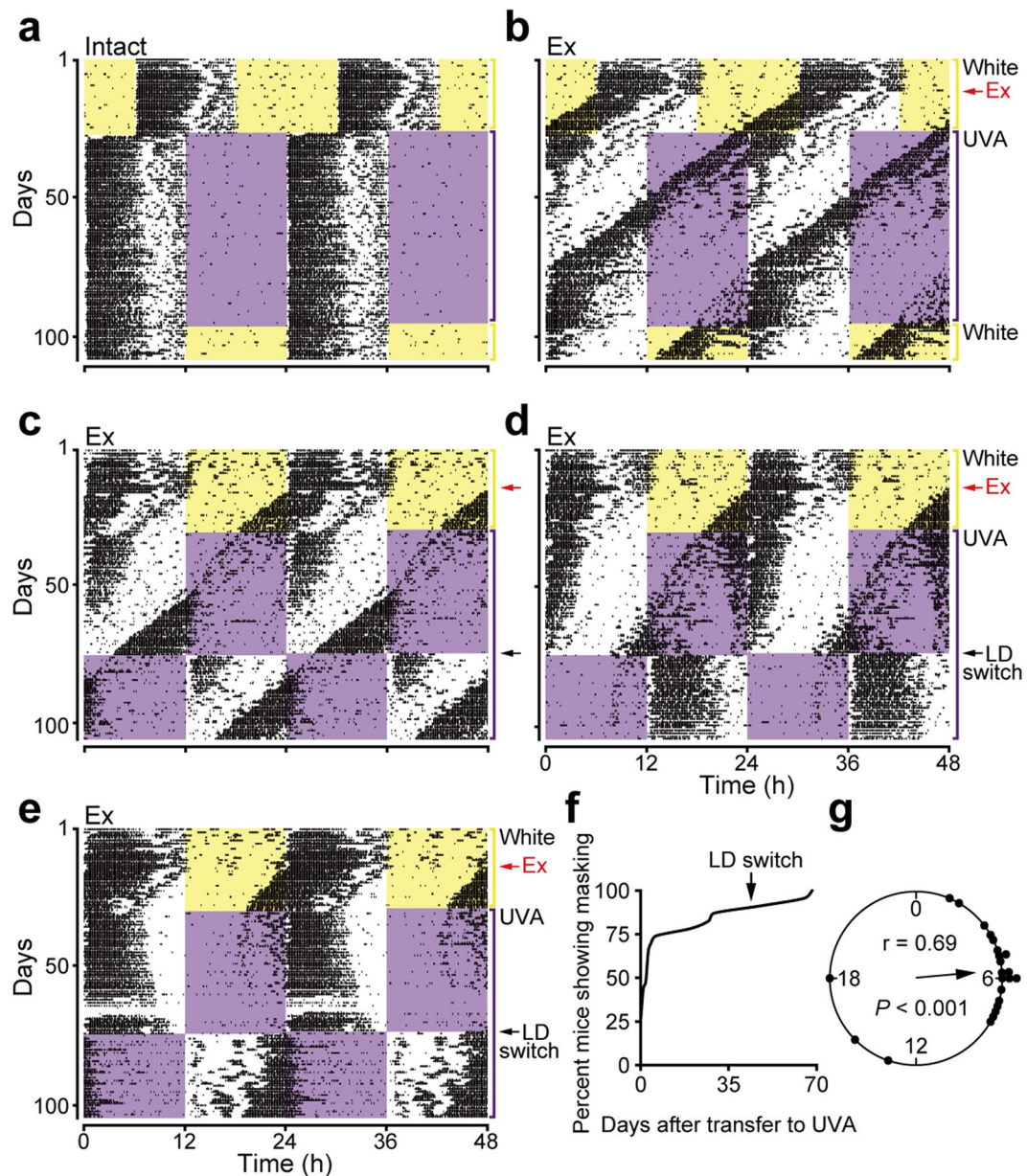
Figure 1. Blinded C57BL/6 J mice exhibit masking behaviors during UVA light exposure. (**a,b**) Representative actograms of intact mice (**a**) and enucleated (Ex) blinded mice. (**b**) The 12-h light periods are shown as colored background (yellow: white light, purple: UVA light [$\lambda_p = 365$ nm]). Ex group mice were bilaterally enucleated on day 14 (Red arrows). (**c–f**) Representative actograms of blinded mice in the validation experiment. (**f**) Percentage of animals exhibiting the negative masking behavior in UVA light phase. (**g**) Rayleigh plot of the phases for the beginning of negative masking behavior. Individual data are plotted on the circle (n = 23). The direction of the arrow indicates the mean phase vector, and the length represents the strength of the phase clustering (*r* value). The *p* value is based on the Rayleigh test.

background of these knockout mice was C57BL/6N, we used C57BL/6N mice as control animals. *Trpv1-*, *Trpv3-*, and *Trpv4-*null mice showed no differences in behavior compared to wild-type mice. However, *Trpm2-* and *Trpm8-*null mice exhibited impaired masking behaviors in response to T_a cycles (Fig. 4a,c). Furthermore, we bred *Trpm2-* and *Trpm8-*null mice to generate double-KO (DKO) mice. Although the observed masking ratio in DKO mice was not significantly different compared to single-KO mice, DKO mice tended to exhibit more severe phenotypes at higher-temperature cycles (e.g., 24/30 °C, 24/32 °C, and 24/34 °C) (Fig. 4b,d). When we compared the total activity of KO mice used in this study, statistically significant differences were only detected in *Trpv4-*null mice at 24/24 °C and 24/26 °C cycles (Supplementary Fig. S3). The low activity observed in *Trpv4-*null mice is likely due to muscular atrophy concomitant with hereditary neuropathies in this mutant[24]. Since we evaluate masking by calculating the activity ratio between different temperatures, the motor dysfunction observed in *Trpv4-*null mice does not affect our results.

Figure 2. Temperature stimulus generated by UVA light causes negative masking behaviors in blinded mice. (**a,b,d,e**) Representative actograms under 3.5/3.5-h LD cycle (**a** White light, **b** UVA light, **d** UVA light + Saline injection under the scalp, **e** UVA light + India ink injection under the scalp). (**c**) Masking ratio under white or UVA light. Mean ± SEM (n = 6; *$p < 0.05$, Student's t-test). (**f**) Masking ratio under white or UVA light, with saline or India ink injection. Mean ± SEM (n = 5–7). (**g,h**) Temperature changes and representative actograms under UVA (**g**) or white (**h**) light–dark conditions.

Possible neural circuit underlying negative masking behavior.   To identify the neural circuit that regulates temperature-dependent masking behavior, we first examined the expression of a histochemical marker of neuronal activation, *Fos*, during temperature-dependent masking behavior by *in situ* hybridization. Thirty minutes of masking-inducing warm temperature stimulus (34 °C) increased *Fos* expression in several nuclei, including the nucleus accumbens (NAc), preoptic area (POA) of the hypothalamus (mainly the median preoptic nucleus [MnPO]), anterior paraventricular nucleus of the thalamus (aPVT), SCN, posterior PVT (pPVT), and dorsomedial nucleus of the hypothalamus (DMH) (Fig. 5a–c). The neural connections among these nuclei are well characterized, and the PVT appears to be an important interface for the regulation of temperature-dependent negative masking behavior (see Discussion). To confirm this hypothesis, we performed chemical lesioning of the aPVT by injecting ibotenate (Fig. 5d–g, Supplementary Figs S4 and S5). Lesion of the entire aPVT was technically impossible due to the high mortality rate caused by repeated injections. However, partial lesions of the aPVT were possible and led to a small (approximately 7%), but significant decrease in temperature-dependent negative masking behavior compared to saline-injected control mice (Fig. 5d–f). Note that total activity did not differ between these two groups (Fig. 5g) and that lesions outside the aPVT had no effect on negative masking behavior (Supplementary Fig. S6). These results suggest that the aPVT is involved in regulation of negative masking behavior.
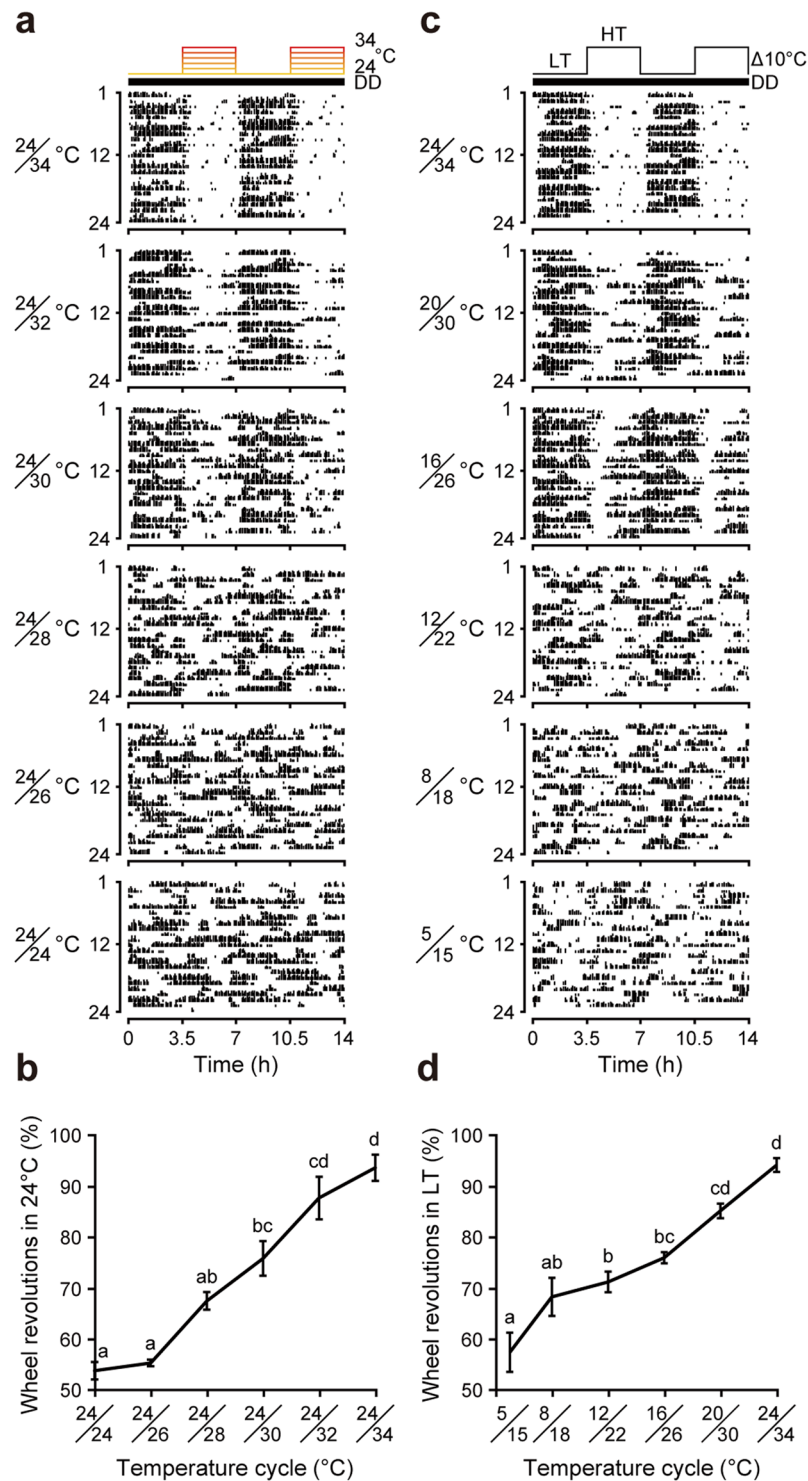
Figure 3. T_a cycles induce negative masking behaviors in mice. (**a**) Representative actograms of C57BL/6J mice. Locomotor activities were recorded for 1 week in DD under various 3.5/3.5-h T_a cycles. Temperature cycle patterns are illustrated at the top. (**b**) Masking ratio under each T_a cycle. Mean ± SEM (n = 4; $p < 0.01$, ANOVA, $F_{5, 23} = 38.94$; $p < 0.01$, Scheffé's *post hoc* test). (**c**) Representative actograms of C57BL/6 J mice in DD under various 3.5/3.5-h T_a cycles in which the temperature difference was held constant at 10 °C. LT: low temperature; HT: high temperature. (**d**) Masking ratio under each 10 °C temperature difference cycle. Mean ± SEM (n = 8; $p < 0.01$, ANOVA, $F_{5, 47} = 26.45$; $p < 0.01$, Scheffé's *post hoc* test). Different letters in (**b**,**d**) indicate significant differences between different groups.
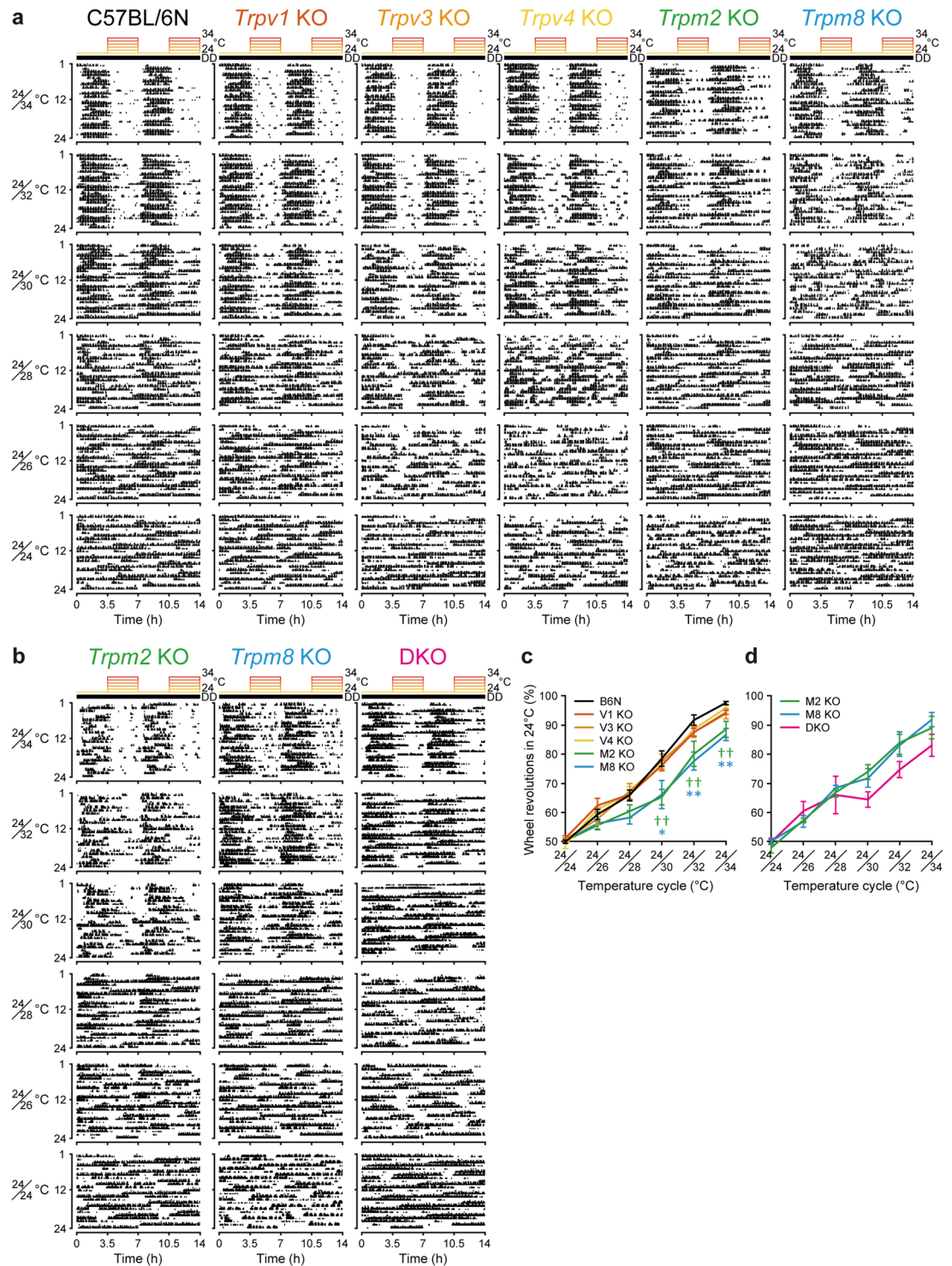
Figure 4. Impaired negative masking behaviors in *Trpm2* KO and *Trpm8* KO mice. (**a**) Representative actograms of C57BL/6 N (B6N), *Trpv1* KO, *Trpv3* KO, *Trpv4* KO, *Trpm2* KO, and *Trpm8* KO mice. (**b**) Representative actograms of *Trpm2* KO, *Trpm8* KO, and *Trpm2/8* DKO mice. (**c**) Masking ratio of each TRP KO mouse shown in (**a**). Mean ± SEM (n = 8–10 [B6N], 7–10 [V1], 6–8 [V3], 3–6 [V4], 5–8 [M2], 5–7 [M8]; ††$p < 0.01$, *a priori* Dunnett's test [B6N vs. *Trpm2* KO]; **$p < 0.01$, *$p < 0.05$, *a priori* Dunnett's test [B6N vs. *Trpm8* KO]). (**d**) Masking ratio of *Trpm2/8* DKO mice shown in (**b**). Mean ± SEM (n = 3–8 [M2], 3–7 [M8], 4–7 [DKO]).

Discussion

In previous studies, we found that UVA-sensitive OPN5-positive cerebrospinal fluid-contacting neurons within the hypothalamus are deep brain photoreceptors that regulate seasonal reproduction in birds[8,9]. Since light penetrates into the brain of small mammals[10] and OPN5 is reportedly expressed in the mammalian brain[11,12], we
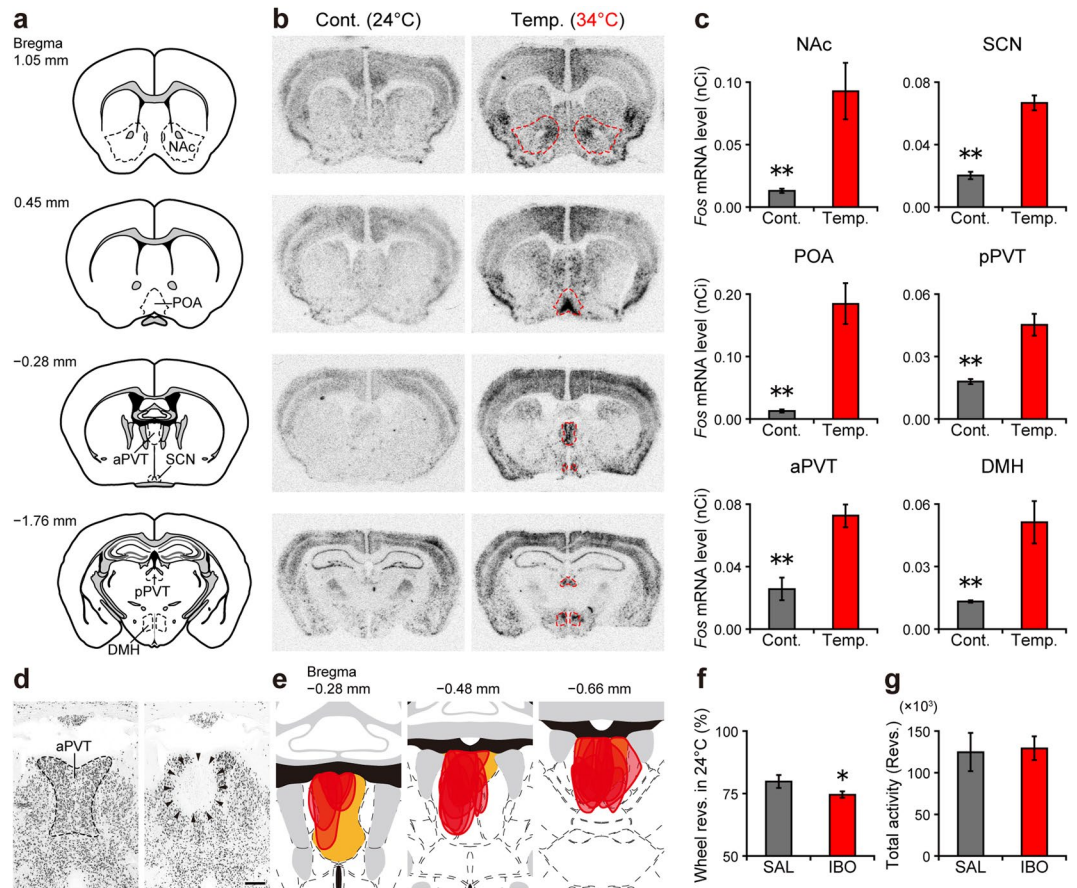
Figure 5. Possible involvement of the aPVT in negative masking behavior. (**a**) Schematic drawings of coronal mouse brain. Black dashed lines indicate the nuclei described in this study. Drawings in (**a,e**) were modified from the mouse brain atlas published by Allen Institute for Brain Science (©2004 Allen Institute for Brain Science. Allen Mouse Brain Atlas. Available from: http://mouse.brain-map.org). (**b**) Representative autoradiograms of *Fos* expression with/without temperature stimulus. Red dashed lines correspond to the black dashed lines in (**a**). (**c**) Densitometric quantifications of each nucleus. Mean ± SEM (n = 4; **$p < 0.01$, Student's *t*-test). (**d**) NeuN immunohistochemistry in the aPVT of saline-injected control (left) and ibotenate-injected aPVT-lesioned (right) mice. Lesioned area is delineated by arrowheads. Scale bar: 200 μm. (**e**) Schematic drawings of aPVT areas lesioned by ibotenate injection (Bregma −0.28 to −0.66 mm). Orange areas indicate the aPVT. Lesioned areas are delineated and translucently filled in red. All lesioned areas and individual data are shown in Supplementary Figs S4 and S5, respectively. (**f,g**) Masking ratio (**f**) and total activity (**g**) of saline-injected control (left) and ibotenate-injected aPVT-lesioned (right) mice. Locomotor activity was recorded for 1 week in DD under a 3.5/3.5-h T$_a$ cycle (24/30 °C). Mean ± SEM (n = 9 [saline], 18 [ibotenate]; *$p < 0.05$, Student's *t*-test).

first examined whether mice have the capacity for extra-ocular photoreception using blinded mice. Although we observed clear suppression of locomotor activity by UVA light exposure (350–400 nm), this behavior was induced by the temperature rise caused by the UVA light source, rather than by UVA light itself (Figs 1 and 2). We therefore conclude that mice do not have the capacity for extra-ocular photoreception as previously suggested[14,15].

Our knowledge of the regulatory mechanisms responsible for masking behavior is significantly less than our understanding of circadian photoentrainment, despite the fact that both phenomena are important for determining the temporal distribution of locomotor activity (i.e., temporal niche). In this study, we observed negative masking-like behavior (i.e., acute suppression of locomotor activity) in mice at higher temperatures, consistent with a previous report[25] (Figs 1–3). When activity was plotted on a 24-h time scale (Supplementary Figs S7 and S8), suppression of locomotor activity was only observed when mice were exposed to the higher temperatures. Importantly, these double-plotted actograms showed that mice were free-running during 3.5/3.5-h T$_a$ cycles (Supplementary Fig. S7) and continued to free-run after transfer from T$_a$ cycles to constant conditions (constant 24 °C with DD) (Supplementary Fig. S8). Thus, the observed suppression of locomotor activity at higher temperatures is clearly negative masking behavior rather than entrainment. In the present study, we evaluated masking behavior by measuring wheel-running activity. One could speculate that animals might reduce their wheel-running activity to prevent hyperthermia at high ambient temperatures and that negative masking behavior depends on the intensity of physical activity. We therefore analyzed total activity during masking behavior (Supplementary Fig. S9). Total activity under 24/34 °C tended to be lower than that of 24/24 °C cycles, but there
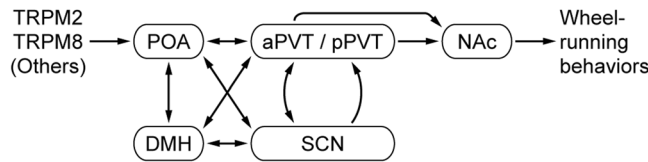
Figure 6. Possible neural circuit regulating temperature-dependent negative masking behavior in mice. Temperature information detected by thermosensors (e.g., TRPM2 and TRPM8) is sent to the thermoregulatory center, the POA, which sends direct and indirect (via DMH and/or SCN) projections to the aPVT/pPVT. The aPVT/pPVT and SCN are reciprocally connected. The aPVT/pPVT sends projections to the NAc, which is involved in the regulation of wheel-running behaviors. Arrows between nuclei indicate direct connections[5,48–56]. Note that TRPM2 is also expressed in the POA[29].

was no significant difference (Supplementary Fig. S9a). By contrast, total activity under 24/34 °C was higher than that at 5/15 °C (Supplementary Fig. S9b). Therefore, we believe that temperature-dependent masking behavior does not necessarily depend on the intensity of the physical activity.

Although several TRPA channels (e.g., dTRPA1 and Pyrexia) are involved in the regulation of activity levels during the afternoon, rhythmicity of temperature preference, and temperature synchronization of the circadian clock in *Drosophila*[26,27], the thermosensors regulating behavioral rhythms in vertebrates remain unknown. Multiple TRP channels covering a wide range of temperatures have been identified in mammals[22,23] (Supplementary Fig. S2). By analyzing all the available TRP channel–knockout mice, we discovered impaired negative masking behaviors in *Trpm2*- and *Trpm8*-null mice (Fig. 4). TRPM2 is a warm-sensitive thermosensor that is activated within the physiological range of body temperature and is involved in the sensation of environmental warmth[28], reduction of fever size by detecting hyperthermic temperature in the POA[29], fever-associated enhancement of macrophage phagocytosis[30], and body temperature–evoked insulin secretion[31]. On the other hand, TRPM8 is a cold-sensitive thermosensor that also acts as a menthol receptor[32,33]. TRPM8 deficiency leads to impairment in sensing unpleasant cold stimuli, including cold-inducing icilin application and acetone cooling[34–36]. Importantly, these two TRP channels are intimately involved in thermoregulation[29,37–39]. Our results demonstrate that warm-sensitive TRPM2 and cold-sensitive TRPM8 also act as thermosensors for the regulation of temperature-dependent negative masking behavior. This seems plausible because to sense absolute temperature value, at least two thermosensors that span different temperature ranges (e.g., cold-sensitive and warm-sensitive channels) are required[40]. However, we do not fully comprehend why both *Trpm2*- and *Trpm8*-null mice showed the same masking behavior within the exact same temperature range. Although *Trpm2*/*Trpm8* DKO mice tend to be more severely impaired than the single-KO mice (Fig. 4b,d), temperature-dependent masking behavior is not abolished. These results are consistent with the fact that individual TRP channel knockout models, and even DKO mice, often do not display strong temperature phenotypes[41]. This is because many TRP channels detect overlapping temperatures, and extensive compensation occurs among redundant temperature detectors. In any case, our data suggests the involvement of additional thermosensor(s) in negative masking behavior. Clearly, further investigation is required to identify these remaining thermosensor(s). Since knockout mice for warm sensitive TRPM4 and TRPM5 were unavailable, they are obvious potential candidates.

Some photoreceptors (i.e., melanopsin [Opn4]-expressing retinal ganglion cells, rods and cones)[6,42–44] and several brain regions (i.e., IGL and olivary pretectal nucleus [OPN])[45,46] are thought to mediate light-dependent masking behavior; however, the brain regions and neural circuits that mediate temperature-dependent masking behavior remain completely unknown. Expression analysis of the neuronal activation marker, *Fos*, reveals that several brain regions (NAc, POA, aPVT, SCN, pPVT, DMH) are activated by an acute increase in T_a that induces negative masking behavior (Fig. 5a–c). The neural connections between these nuclei are well characterized. Environmental temperature detected by thermosensors located in the skin and the brain is transmitted to the POA, the mammalian thermoregulatory center[47]. The POA, PVT, DMH, and SCN are mutually connected[5,48–55]. Direct[49–52] and indirect projections through the DMH[48–52] or the SCN[5,49–55] connect the POA to the PVT. The PVT is reciprocally connected with the SCN; aPVT neurons send projections to the SCN, and SCN neurons project to the aPVT and pPVT[5,49–55]. The aPVT and pPVT send dense projections to the NAc[50–53,56], an area of the striatum that acts as a limbic–motor interface to mediate a variety of behaviors, including motivation, locomotion, reward, and wheel-running activity[57–59]. Notably, in this regard, wheel-running is considered a reward to rodents[60]. Thus, the PVT appeared to be an important interface for the regulation of temperature-dependent negative masking behavior. Interestingly, we observed a slight decrease in masking behavior by partial lesion of the aPVT, suggesting the possible involvement of this nucleus in the regulation of negative masking behavior (Fig. 5d–f). Based on these findings, we propose a neural circuit responsible for regulating temperature-dependent negative masking behavior in mice (Fig. 6).

Recent studies have shown that the behavior of animals differs markedly between laboratory conditions (rectangular light/dark cycles and constant warm temperature) and natural conditions (gradually changing light intensity and temperature)[61–66]. Entrainment and masking are two independent processes that determine the timing of activity (temporal niche). Although a great deal of effort has been devoted to understanding the mechanisms underlying photoentrainment, the mechanisms responsible for masking behavior have remained unknown. We report here that two thermosensors, TRPM2 and TRPM8, are involved in the regulation of temperature-dependent negative masking behavior. Moreover, the PVT is likely to be an important interface for this adaptive behavior. We believe that our findings will contribute to a greater understanding of masking

behavior, and eventually, to the regulatory mechanisms involved in temporal niche switching (e.g., diurnality and nocturnality).

Methods

Animals. C57BL/6J and C57BL/6N mice were purchased from a local dealer (Japan SLC, Inc.). TRP channel KO mice (*Trpv1*[67], *Trpv3*[68], *Trpv4*[69], *Trpm2*[70], *Trpm8*[35]) backcrossed more than 5 times with C57BL/6N mice were used in this study. *Trpm2/Trpm8* DKO mice (F2 progeny) generated by intercrosses between *Trpm2* KO mice and *Trpm8* KO mice were also used in this study. We used male mice whenever possible. If sufficient numbers of males were not available, we used female mice: *Trpv1* KO (4 females out of 10) and *Trpm8* KO (3 females out of 7) mice in Fig. 4c; *Trpm2* KO (5 females out of 8), *Trpm8* KO (5 females out of 7) and *Trpm2/Trpm8* DKO (5 females out of 7) mice in Fig. 4d. The total number of male and female mice was too small for a proper statistical comparison, and further detailed analyses are required to confirm any sex differences. However, of the mice used in this study, no clear differences were observed between the sexes. All animals were housed in a controlled environment (white-LD cycle [12/12-h]; room temperature 22–24 °C) prior to experiments. Food and water were provided *ad libitum*. All animal procedures in this study were approved by the Animal Experiment Committee of Nagoya University, and all experiments were performed in accordance with the relevant guidelines and regulations.

Effect of UVA light exposure on wheel-running activity of blinded mice. Eight-week-old male C57BL/6J mice were kept in individual cages (14.8 × 25.0 × 14.8 cm) equipped with running wheels (10.0 cm diameter), and the cages were placed together in a light-tight box (136.7 × 42.5 × 42.5 cm). Light in the box was provided by fluorescent lamps (white light: FHF32EX-N-H, Panasonic, 4,150 lux at the top of the cage; UVA light: TL-D 36 W/08 low-pressure mercury vapor fluorescent lamp, Philips, peak wavelength 365 nm with half-bandwidth 13.9 nm). Both eyes were surgically removed (enucleated) under isoflurane anesthesia (Ex group). Two weeks after the surgery, the light source was changed to UVA light (light intensity ~15.3 log photons $cm^{-2} s^{-1}$, less than the intensity under direct sunlight in Nagoya, Japan). Wheel-running activities were continuously recorded using the Chronobiology Kit (Stanford Software Systems). T_a in the light-tight box was measured using temperature data loggers (Thermochron type-G, KN Laboratories), and data were retrieved using the ThermoManager software (KN Laboratories).

Evaluation of masking behavior. A 3.5/3.5-h LD cycle and a T_a cycle were used to quantitatively evaluate masking behavior (Supplementary Fig. S1). The number of wheel revolutions in the dark- or lower temperature-phase compared to the total number of revolutions was defined as the masking ratio. When the animal's activity is unaffected by environmental stimuli, the masking ratio is close to 50%. A Biomulti incubator (LP-30CCFL-8CTAR, Nippon Medical & Chemical Instruments) was used for temperature control. Using this equipment, we could control the T_a and light conditions independently. T_a cycles were examined in the following order: 24/28 °C, 24/30 °C, 24/32 °C, 24/34 °C, 24/24 °C, 24/26 °C.

India ink injection under the scalp. India ink (Tenboku, Kuretake) was autoclaved the day before injection. Autoclaved India ink (300 µl) was injected between the scalp and the skull of mice using a 1-ml syringe and 26 G needle under isoflurane anesthesia. The same amount of saline was injected into the control group.

***In situ* hybridization of *Fos* mRNA.** Eight-week-old male C57BL/6N mice were placed in individual cages equipped with running wheels and were entrained to a white-LD cycle (12/12-h) for 2 weeks. During this time, the T_a was maintained at 24 °C. Subsequently, a 30-min warm-temperature stimulus (34 °C) was given 4-hour after the light offset (Zeitgeber time [ZT] 16) in the temperature stimulus group (Fig. 5b-right). In the control group, T_a was held constant at 24 °C (Fig. 5b-left). Because *Fos* mRNA expression peaks 30 minutes after stimulation[71], brains were collected using a pair of night-vision goggles (Ninox, Armasight) and rapidly frozen in dry ice at ZT16.5. Non-perfused frozen sections (20-µm thickness) were prepared using a cryostat (CM3050 S, Leica Microsystems) and examined with ^{33}P-labeled oligonucleotide probes. Four 45-mer oligonucleotide probes were designed against the mouse *Fos* gene (GenBank: NM_010234) and used as a mixture to increase the sensitivity. Hybridization was carried out overnight at 42 °C. Two high-stringency post-hybridization washes were performed at 55 °C. Sections were air-dried and exposed to BioMax MR Film (Eastman Kodak) for 4 weeks with ^{14}C-Standard slide (American Radiolabeled Chemicals). Densitometric quantification of hybridization signals was performed using the Multi Gauge software (Fujifilm). The probe sequences were as follows:

5′-tcactgctcgttcgcggaaccgccggctctatccagtcttctcag-3′
5′-tccaggggaggccacagacatctcctctgggaagccaaggtcatcg-3′
5′-atctggcacagagcgggaggtctctgagccactgggcctagatga-3′
5′-ctggaggccagatgtggatgcttgcaagtccttgaggcccacagc-3′

Ibotenate injection into the aPVT. Ibotenate injection was performed in accordance with the earlier study[72]. Mice were deeply anesthetized with chloral hydrate (280 mg kg^{-1}, i.p. injection with 7% solution). Subsequently, 5 mM ibotenate or saline (20–50 nl) was injected to the aPVT (coordinates: 0.2 mm caudal to bregma, 0.0 mm lateral to the midline, and 3.6 mm ventral to the skull surface). Due to the high mortality rate, each mouse received only one injection. Lesioned areas were evaluated by NeuN immunohistochemistry immediately after evaluation of masking behavior, and are depicted in Fig. 5e, Supplementary Figs S4 and S5. All behavioral analyses of ibotenate- or saline-injected mice were performed after >1 week of recovery.

Immunohistochemistry.   Immunohistochemistry was performed using rabbit monoclonal anti-NeuN antibody (ab177487, Abcam) (dilution 1:500) and N-Histofine Simple Stain Mouse MAX PO (R) (Nichirei Biosciences) with a standard protocol[73].

Statistical analysis.   All data are shown as the mean ± SEM. Statistical analyses were performed using the Rayleigh test, Student's t-test, or one-way ANOVA, followed by Scheffé's *post hoc* test or *a priori* Dunnett's test.

Data Availability

Any related data and/or information of this study are available from the corresponding author upon request.

References

1. Aschoff, J. Masking of circadian rhythms by zeitgebers as opposed to entrainment. In *Trends in Chronobiology* (eds Hekkens, W. T. J. M., Kerkhof, G. A. & Rietveld, W. J.) 149–161 (Pergamon Press, 1988).
2. Mrosovsky, N. Masking: History, definitions, and measurement. *Chronobiol. Int.* **16**, 415–429 (1999).
3. Klein, D. C., Moore, R. Y. & Reppert, S. M. *Suprachiasmatic nucleus: The mind's clock.* (Oxford Univ. Press, 1991).
4. Pickard, G. E., Ralph, M. R. & Menaker, M. The intergeniculate leaflet partially mediates effects of light on circadian rhythms. *J. Biol. Rhythms* **2**, 35–56 (1987).
5. Moga, M. M. & Moore, R. Y. Organization of neural inputs to the suprachiasmatic nucleus in the rat. *J. Comp. Neurol.* **534**, 508–534 (1997).
6. Hattar, S. *et al.* Melanopsin and rod-cone photoreceptive systems account for all major accessory visual functions in mice. *Nature* **424**, 76–81 (2003).
7. von Frisch, K. Beiträge zur physiologie der pigmentzellen in der fischhaut. *Pflüger's, Arch. Gesammte Physiol. Menschen Tiere* **138**, 319–387 (1911).
8. Nakane, Y. *et al.* A mammalian neural tissue opsin (Opsin 5) is a deep brain photoreceptor in birds. *Proc. Natl. Acad. Sci. USA* **107**, 15264–15268 (2010).
9. Nakane, Y., Shimmura, T., Abe, H. & Yoshimura, T. Intrinsic photosensitivity of a deep brain photoreceptor. *Curr. Biol.* **24**, R596–R597 (2014).
10. Hartwig, H. G. & van Veen, T. Spectral characteristics of visible radiation penetrating into the brain and stimulating extraretinal photoreceptors. *Journal of Comparative Physiology* **130**, 277–282 (1979).
11. Tarttelin, E. E., Bellingham, J., Hankins, M. W., Foster, R. G. & Lucas, R. J. Neuropsin (Opn5): a novel opsin identified in mammalian neural tissue. *FEBS Lett.* **554**, 410–416 (2003).
12. Yamashita, T. *et al.* Evolution of mammalian Opn5 as a specialized UV-absorbing pigment by a single amino acid mutation. *J. Biol. Chem.* **289**, 3991–4000 (2014).
13. Kojima, D. *et al.* UV-sensitive photoreceptor protein OPN5 in humans and mice. *PLoS One* **6**, e26388 (2011).
14. Groos, G. A. & van der Kooy, D. Functional absence of brain photoreceptors mediating entrainment of circadian rhythms in the adult rat. *Experientia* **37**, 71–72 (1981).
15. Nelson, R. J. & Zucker, I. Absence of extraocular photoreception in diurnal and nocturnal rodents exposed to direct sunlight. *Comp. Biochem. Physiol. Part A Physiol.* **69**, 145–148 (1981).
16. Yamazaki, S., Alones, V. & Menaker, M. Interaction of the retina with suprachiasmatic pacemakers in the control of circadian behavior. *J. Biol. Rhythms* **17**, 315–329 (2002).
17. Hoffmann, K. Die relative wirksamkeit von zeitgebern (The relative effectiveness of zeitgebers). *Oecologia* **3**, 184–206 (1969).
18. Redlin, U. & Mrosovsky, N. Masking of locomotor activity in hamsters. *J. Comp. Physiol. A.* **184**, 429–437 (1999).
19. Menaker, M., Roberts, R., Elliott, J. & Underwood, H. Extraretinal light perception in the sparrow, III: The eyes do not participate in photoperiodic photoreception. *Proc. Natl. Acad. Sci. USA* **67**, 320–325 (1970).
20. Gordon, C. J. *Temperature regulation in laboratory rodents.* (Cambridge University Press, 1993).
21. Gaskill, B. N., Rohr, S. A., Pajor, E. A., Lucas, J. R. & Garner, J. P. Some like it hot: Mouse temperature preferences in laboratory housing. *Appl. Anim. Behav. Sci.* **116**, 279–285 (2009).
22. Kashio, M. & Tominaga, M. Thermo-sensitive TRP channel sensing body temperature. in Experimental Medicine 512–518 (Yodosha, 2014).
23. Kashio, M. & Tominaga, M. The TRPM2 channel: A thermo-sensitive metabolic sensor. *Channels* **11**, 426–433 (2017).
24. Zimon, M. *et al.* Dominant mutations in the cation channel gene transient receptor potential vanilloid 4 cause an unusual spectrum of neuropathies. *Brain* **133**, 1798–1809 (2010).
25. Francis, A. J. & Coleman, G. J. The effect of ambient temperature cycles upon circadian running and drinking activity in male and female laboratory rats. *Physiol. Behav.* **43**, 471–477 (1988).
26. Bellemer, A. Thermotaxis, circadian rhythms, and TRP channels in *Drosophila*. *Temperature* **2**, 227–243 (2015).
27. Roessingh, S. & Stanewsky, R. The *Drosophila* TRPA1 channel and neuronal circuits controlling rhythmic behaviours and sleep in response to environmental temperature. *Int. J. Mol. Sci.* **18**, E2028 (2017).
28. Tan, C. H. & McNaughton, P. A. The TRPM2 ion channel is required for sensitivity to warmth. *Nature* **536**, 460–463 (2016).
29. Song, K. *et al.* The TRPM2 channel is a hypothalamic heat sensor that limits fever and can drive hypothermia. *Science* **353**, 1393–1398 (2016).
30. Kashio, M. *et al.* Redox signal-mediated sensitization of transient receptor potential melastatin 2 (TRPM2) to temperature affects macrophage functions. *Proc. Natl. Acad. Sci. USA* **109**, 6745–6750 (2012).
31. Togashi, K. *et al.* TRPM2 activation by cyclic ADP-ribose at body temperature is involved in insulin secretion. *EMBO J.* **25**, 1804–1815 (2006).
32. McKemy, D. D., Neuhausser, W. M. & Julius, D. Identification of a cold receptor reveals a general role for TRP channels in thermosensation. *Nature* **416**, 52–58 (2002).
33. Peier, A. M. *et al.* A TRP channel that senses cold stimuli and menthol. *Cell* **108**, 705–715 (2002).
34. Colburn, R. W. *et al.* Attenuated cold sensitivity in TRPM8 null mice. *Neuron* **54**, 379–386 (2007).
35. Dhaka, A. *et al.* TRPM8 is required for cold sensation in mice. *Neuron* **54**, 371–378 (2007).
36. Bautista, D. M. *et al.* The menthol receptor TRPM8 is the principal detector of environmental cold. *Nature* **448**, 204–208 (2007).
37. Gavva, N. R. *et al.* Transient receptor potential melastatin 8 (TRPM8) channels are involved in body temperature regulation. *Mol. Pain* **8**, 36 (2012).
38. Almeida, M. C. *et al.* Pharmacological blockade of the cold receptor TRPM8 attenuates autonomic and behavioral cold defenses and decreases deep body temperature. *J. Neurosci.* **32**, 2086–2099 (2012).
39. Reimúndez, A. *et al.* Deletion of the cold thermoreceptor TRPM8 increases heat loss and food intake leading to reduced body temperature and obesity in mice. *J. Neurosci.* **38**, 3643–3656 (2018).
40. Patapoutian, A., Peier, A. M., Story, G. M. & Viswanath, V. ThermoTRP channels and beyond: Mechanisms of temperature sensation. *Nat. Rev. Neurosci.* **4**, 529–539 (2003).
41. Wang, H. & Siemens, J. TRP ion channels in thermosensation, thermoregulation and metabolism. *Temperature* **2**, 178–187 (2015).

42. Mrosovsky, N. & Hattar, S. Impaired masking responses to light in melanopsin-knockout mice. *Chronobiol. Int.* **20**, 1–11 (2003).
43. Mrosovsky, N., Foster, R. G. & Salmon, P. A. Thresholds for masking responses to light in three strains of retinally degenerate mice. *J. Comp. Physiol. A* **184**, 423–428 (1999).
44. Mrosovsky, N. & Hattar, S. Diurnal mice (*Mus musculus*) and other examples of temporal niche switching. *J. Comp. Physiol. A* **191**, 1011–1024 (2005).
45. Gall, A. J., Smale, L., Yan, L. & Nunez, A. A. Lesions of the intergeniculate leaflet lead to a reorganization in circadian regulation and a reversal in masking responses to photic stimuli in the Nile grass rat. *PLoS One* **8**, e67387 (2013).
46. Gall, A. J. *et al.* Normal behavioral responses to light and darkness and the pupillary light reflex are dependent upon the olivary pretectal nucleus in the diurnal Nile grass rat. *Neuroscience* **355**, 225–237 (2017).
47. Nakamura, K. Central circuitries for body temperature regulation and fever. *Am. J. Physiol. Regul. Integr. Comp. Physiol.* **301**, R1207–R1228 (2011).
48. Kita, H. & Oomura, Y. An HRP study of the afferent connections to rat medial hypothalamic region. *Brain Res. Bull.* **8**, 53–62 (1982).
49. Chen, S. & Su, H. S. Afferent connections of the thalamic paraventricular and parataenial nuclei in the rat–a retrograde tracing study with iontophoretic application of Fluoro-Gold. *Brain Res.* **522**, 1–6 (1990).
50. Li, S. & Kirouac, G. J. Sources of inputs to the anterior and posterior aspects of the paraventricular nucleus of the thalamus. *Brain Struct. Funct.* **217**, 257–273 (2012).
51. Colavito, V., Tesoriero, C., Wirtu, A. T., Grassi-Zucconi, G. & Bentivoglio, M. Limbic thalamus and state-dependent behavior: The paraventricular nucleus of the thalamic midline as a node in circadian timing and sleep/wake-regulatory networks. *Neurosci. Biobehav. Rev.* **54**, 3–17 (2015).
52. Kirouac, G. J. Placing the paraventricular nucleus of the thalamus within the brain circuits that control behavior. *Neurosci. Biobehav. Rev.* **56**, 315–329 (2015).
53. Moga, M. M., Weis, R. P. & Moore, R. Y. Efferent projections of the paraventricular thalamic nucleus in the rat. *J. Comp. Neurol.* **359**, 221–238 (1995).
54. Watts, A. G., Swanson, L. W. & Sanchez-Watts, G. Efferent projections of the suprachiasmatic nucleus: I. Studies using anterograde transport of *Phaseolus vulgaris* leucoagglutinin in the rat. *J. Comp. Neurol.* **258**, 204–229 (1987).
55. Watts, A. G. & Swanson, L. W. Efferent projections of the suprachiasmatic nucleus: II. Studies using retrograde transport of fluorescent dyes and simultaneous peptide immunohistochemistry in the rat. *J Comp Neurol* **258**, 230–252 (1987).
56. Hsu, D. T., Kirouac, G. J., Zubieta, J. K. & Bhatnagar, S. Contributions of the paraventricular thalamic nucleus in the regulation of stress, motivation, and mood. *Front. Behav. Neurosci.* **8**, 1–10 (2014).
57. Mogenson, G. J., Jones, D. L. & Yim, C. Y. From motivation to action: Functional interface between the limbic system and the motor system. *Prog. Neurobiol.* **14**, 69–97 (1980).
58. Roberts, M. D. *et al.* Nucleus accumbens neuronal maturation differences in young rats bred for low versus high voluntary running behaviour. *J. Physiol.* **592**, 2119–2135 (2014).
59. Basso, J. C. & Morrell, J. I. The medial prefrontal cortex and nucleus accumbens mediate the motivation for voluntary wheel running in the rat. *Behav. Neurosci.* **129**, 457–472 (2015).
60. Novak, C. M., Burghardt, P. R. & Levine, J. A. The use of a running wheel to measure activity in rodents: Relationship to energy balance, general activity, and reward. *Neurosci. Biobehav. Rev.* **36**, 1001–1014 (2012).
61. Vanin, S. *et al.* Unexpected features of *Drosophila* circadian behavioural rhythms under natural conditions. *Nature* **484**, 371–375 (2012).
62. Gattermann, R. *et al.* Golden hamsters are nocturnal in captivity but diurnal in nature. *Biol. Lett.* **4**, 253–255 (2008).
63. Calisi, R. M. & Bentley, G. E. Lab and field experiments: Are they the same animal? *Horm. Behav.* **56**, 1–10 (2009).
64. Daan, S. *et al.* Lab mice in the field: Unorthodox daily activity and effects of a dysfunctional circadian clock allele. *J. Biol. Rhythms* **26**, 118–129 (2011).
65. Hut, R. A., Kronfeld-Schor, N., Van der Vinne, V. & De la Iglesia, H. In search of a temporal niche: Environmental factors. *Prog. Brain Res.* **199**, 281–304 (2012).
66. van der Veen, D. R. *et al.* Flexible clock systems: Adjusting the temporal programme. *Phil. Trans. R. Soc. B* **372**, 20160254 (2017).
67. Caterina, M. J. *et al.* Impaired nociception and pain sensation in mice lacking the capsaicin receptor. *Science* **288**, 306–313 (2000).
68. Moqrich, A. *et al.* Impaired thermosensation in mice lacking TRPV3, a heat and camphor sensor in the skin. *Science* **307**, 1468–1472 (2005).
69. Suzuki, M., Mizuno, A., Kodaira, K. & Imai, M. Impaired pressure sensation in mice lacking TRPV4. *J. Biol. Chem.* **278**, 22664–22668 (2003).
70. Yamamoto, S. *et al.* TRPM2-mediated Ca^{2+} influx induces chemokine production in monocytes that aggravates inflammatory neutrophil infiltration. *Nat. Med.* **14**, 738–747 (2008).
71. Radzioch, D., Bottazzi, B. & Varesio, L. Augmentation of *c-fos* mRNA expression by activators of protein kinase C in fresh, terminally differentiated resting macrophages. *Mol. Cell. Biol.* **7**, 595–599 (1987).
72. Yahiro, T., Kataoka, N., Nakamura, Y. & Nakamura, K. The lateral parabrachial nucleus, but not the thalamus, mediates thermosensory pathways for behavioural thermoregulation. *Sci. Rep.* **7**, 5031 (2017).
73. Ota, W., Nakane, Y., Hattar, S. & Yoshimura, T. Impaired circadian photoentrainment in *Opn5*-null mice. *iScience* **6**, 299–305 (2018).

Acknowledgements

Author Contributions

T.Y. and W.O. designed research; W.O. performed research; Y.N., M.K., Y.S., K.N., Y.M. and M.T. contributed new reagents/analytic tools; W.O. and T.Y. analyzed data; W.O. and T.Y. wrote the paper; all authors commented on the paper.

Additional Information

Supplementary information accompanies this paper at https://doi.org/10.1038/s41598-019-40067-x.

Competing Interests: The authors declare no competing interests.

Publisher's note: Springer Nature remains neutral with regard to jurisdictional claims in published maps and institutional affiliations.